

Schottky Barrier MOSFET Enabled Ultra-Low Power Real-Time Neuron for Neuromorphic Computing

Shubham Patil, Jayatika Sakhuja, Ajay Kumar Singh, Anmol Biswas, Vivek Saraswat, Sandeep Kumar, Sandip Lashkare, Udayan Ganguly
Electrical Engineering, IIT Bombay, Bombay, India. Email: udayan@ee.iitb.ac.in

Abstract

Energy-efficient real-time synapses and neurons are essential to enable large-scale neuromorphic computing. In this paper, we propose and demonstrate the Schottky-Barrier MOSFET-based ultra-low power voltage-controlled current source to enable real-time neurons for neuromorphic computing. Schottky-Barrier MOSFET is fabricated on a Silicon-on-insulator platform with polycrystalline Silicon as the channel and Nickel/Platinum as the source/drain. The Poly-Si and Nickel make the back-to-back Schottky junction enabling ultra-low ON current required for energy-efficient neurons.

Introduction

In the internet of things (IoT) era, data-centric computation is gaining significant interest due to its high energy efficiency. The traditional computers are based on von Neumann architecture, where data and processing units are located separately. Hence, there is significant energy consumption during data transfer between memory and processing unit [1].

Among various alternate technologies, neuromorphic computing is gaining significant interest as its architecture is inspired from the human brain, where memory and processing units are not separate. A spiking neural network (SNN) is a 3rd generation neural network that offers energy-efficient computation by realizing brain functionalities [2]. Synapses and neurons are the basic building blocks of the SNN [3]. Various silicon and non-silicon-based synapse and neuron demonstrations exist in the literature [4-6]. Though the main functionality of synapse and neuron is demonstrated, a complete circuit realization requires the current-to-voltage (V(I)) converter in the synapse implementation. The I-V converter ensures that the synapse type and array are neuron-design-independent by avoiding the loading effect. Similarly, Voltage controlled current source (I(V)) is required in the neuron implementation, which makes the neuron independent of synapse type and array. Hence, the I(V) and V(I) are essential to make both the synapse and neuron modular (Fig. 1).

The Voltage controlled current source (I(V)) is generally implemented by applying the voltage to a typical metal oxide semiconductor field effect transistor (MOSFET). However, the ON currents (mA) of the MOSFET are very large, making the neuron very fast (MHz) (as compared to <kHz for

biological neurons) [5]. To lower the power consumption, the sub-threshold region of MOSFET is utilized with low ON current [7]. However, this makes the V-I conversion non-linear making adding additional circuit requirements on neurons (Table 1). To resolve this challenge, in this paper, we propose and demonstrate a Schottky barrier (SB) MOSFET for a voltage-dependent ultra-low current source (I(V)) for power-efficient real-time neurons.

In this paper, first, we demonstrate the SB-MOSFET on the SOI platform with Gd₂O₃ as box oxide. The polycrystalline Silicon is used as channel material, and Nickel (Ni)/Platinum (Pt) is used as a source/drain to make the Schottky barrier. Next, we demonstrate the SB limited ultra-low current controlled by the top and bottom gate voltage. Finally, a real-time neuron (<kHz) is demonstrated using the ultra-low current output from the SB MOSFET, and a Spiking Neural Network (SNN) is demonstrated to show software equivalent learning accuracy. Such a voltage to the ultra-low current device is essential to implement a real-time neural network that can effectively mimic human brain functionality to solve intricate real-time applications.

Device Fabrication and characterization

The fabricated SB MOSFET schematic and the detailed process flow are shown in Fig. 2. First, the epitaxial Gd₂O₃ layer is deposited on Si (111) with resistivity 0.001 Ω -cm in the RF magnetron sputter of AJA International using a Gd₂O₃ target with 99.999% purity [8]. Second, the active area is defined using the deposition and lift-off of an undoped Si layer (~40 nm) using RF sputtering. Next, the sample is exposed to rapid thermal annealing (RTA) at 400 °C/1 min in N₂ ambient to improve the mobility of the channel layer. Third, Source and drain are defined using Ni/Pt stack deposition and lift-off using AJA 6-target e-beam evaporator. Forth, the high-k Hafnium oxide (HfO₂, 16 nm) as gate insulator is deposited using atomic layer deposition (ALD), followed by gate metal (Tungsten (W)) deposition using DC sputtering. Finally, the S/D contact pads are defined by wet etching of HfO₂ using BHF.

The fabricated structure is structurally and electrically characterized. The surface HRSEM image of the fabricated SB MOSFET is shown in Fig. 3. The devices with gate lengths (L_G) of 10, 20, 25, and 75 μ m with fixed Width (W) = 33 μ m are used in this work. The capacitor with a value of 10 pF and 4.7

nF is used for neuron characterization.

Results and discussions

A. Electrical characterization

I. Transfer and output characteristics: Fig. 4 shows the transfer (Fig. 4a) and output characteristics (Fig. 4b) of the SB MOSFET for $L_G/W = 20/33 \mu\text{m}$ using the Si (p++) substrate as the back gate (BG) with Gd_2O_3 oxide. We observe the good back gate control with low leakage current (pA) through the oxide (Fig. 4c), confirming its good quality. Fig. 5 shows the transfer (Fig. 5a) and output characteristics (Fig. 5b) of the SB MOSFET for $L_G/W = 10/33 \mu\text{m}$ with top gate (TG) control with HfO_2 as a gate oxide. We have shown typical control of a MOSFET with current limited by SB with V_{GS} and V_{DS} dependence. Next, the extracted device performance parameters, (a) g_m (Fig. 5c), (b) μ_{eff} (Fig. 5d), and (c) R_{SD} (Fig. 5e), are shown. The low current of fabricated MOSFET is due to (1) the Schottky barrier at the S/D end and (2) the high resistivity of the Silicon channel layer.

Next, we have shown the drain current tunability using the back gate bias (V_{BG}) for a fixed top gate bias (V_{TG}), as shown in Fig. 6a. This shows the threshold voltage tuning of the MOSFET with BG bias. Furthermore, Fig. 6b shows the impact of L_G scaling on device performance. Drain current is inversely proportional with L_G as typical to traditional bulk MOSFET (Fig. 6c). This fabricated “voltage-dependent ultra-low current source” can enable compact and energy-efficient Neuromorphic architectures. Next, we show neuronal behavior.

II. Neuron demonstration: The circuit used for the neuron demonstration is shown in Fig. 7a. The voltage measurement across the capacitor directly using oscilloscopes is challenging, as it has a low maximum impedance (1 M Ω). To circumvent this problem, the measurement is carried out using a buffer (input resistance > 10 T Ω) between (C) of 4.7 nF is used for this measurement. Fig. 7b shows the output voltage (V_{out}) versus time for different V_{TG} s at

fixed $V_D = 1.5\text{V}$. The capacitor charging time decreases with an increase in V_{TG} . The extracted frequency versus V_{TG} is shown in Fig. 7c for (1) $V_D = 1.5 \text{ V}$ and 2.5 V at fixed $C = 4.7\text{nF}$ and (2) for two different C values of 10 pF and 4.7 nF at $V_D = 2.5 \text{ V}$. The threshold voltage (V_{th}) is set at 0.6 V . We observe the frequency tunability with a change in V_D . Further, $\sim 5.4\text{x}$ frequency improvement is shown for the 10 pF case. Hence, we demonstrate the real-time neuron (<kHz) akin to biological neuron frequency using the ultra-low current output from the SB MOSFET. Next, we implemented a two-layer feedforward (16×3) SNN using a supervised learning algorithm with Leaky Integrate and Fire (LIF) neurons and plastic synapses in MATLAB to solve Fisher’s Iris classification problem [3]. The gate voltage (V_{TG})-dependent SB current is modeled by a voltage-dependent current source ($I_{in} = f(V_{TG})$) (Fig. 7d). A software equivalent accuracy of 96.7% is shown as compared to the ideal LIF neuron for the Fisher Iris classification data (Fig. 7e).

Conclusion

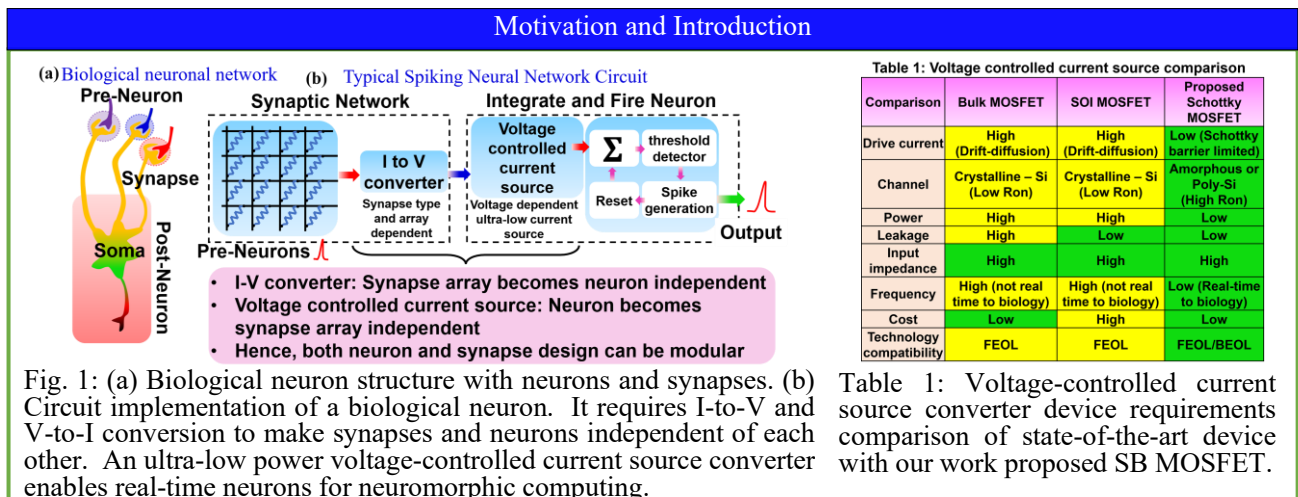
We demonstrated the SB-MOSFET with ultra-low current controlled by the top and bottom gate voltage on the SOI platform with Gd_2O_3 as box oxide. The ultra-low current output from the SB MOSFET was used to demonstrate the real-time neuron (<kHz) akin to biological neuron frequency. Low controllable current sources are critical to reduce the capacitive area for implementing the sub-kHz time scale neurons for processing real-world signals.

Acknowledgment

This work is partially supported by DST and MeitY.

References

- [1] X. Zou, *et al.*, *Sci. China Inf. Sci.*, Vol. 64, 2021. [2] W. Maass, *et al.*, *Neural Netw.*, 10 (9), 1659–1671, 1997. [3] T. Chavan, *et al.*, *IEEE TED*, Vol. 67, no. 4, pp. 2614-2620, 2020. [4] P. Merolla, *et al.*, *IEEE CICC*, pp. 1-4, 2011. [5] S. Dutta, *IEEE TED*, Vol. 7, no. 1, pp. 1-7, 2017. [6] I. Sourikopoulos *et al.*, *Frontiers Neurosci.*, Vol. 11, pp. 123, 2017. [7] T. Chavan *et al.*, *IEEE DRC*, pp. 1-2, 2018. [8] A. Rawat, *TSF*, Vol. 742, 2022.



Fabrication and physical characterization

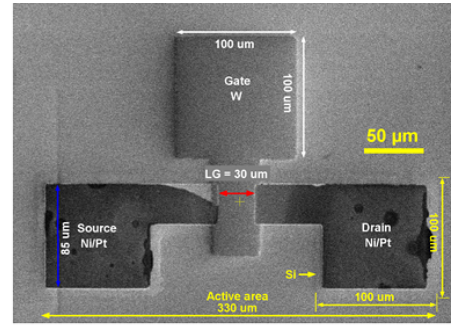
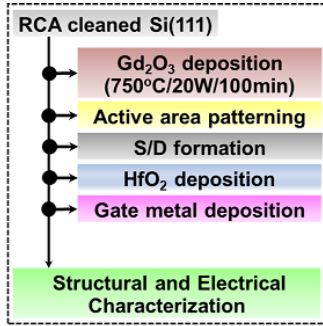
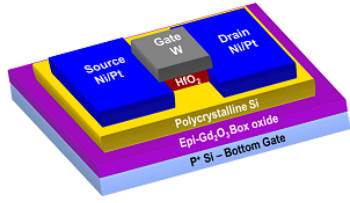


Fig. 2: Schematic and process flow of the fabricated SB MOSFET used in this work. Ni/Pt stack is used as S/D contact.

Fig. 3: Surface scanning electron microscope (SEM) image of the fabricated SB MOSFET.

Electrical characterization: Ultra Low Current SB MOSFET

Back Gate (BG) control

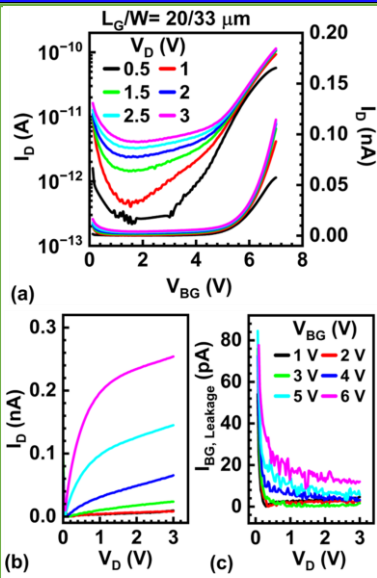


Fig. 4 (a) I_D - V_{BG} , (b) I_D - V_D , and (c) $I_{BG,Leakage}$ - V_D of the MOSFET with back gate (BG). Good gate control with low box oxide leakage current (pA) confirming its good quality.

Top Gate (TG) control

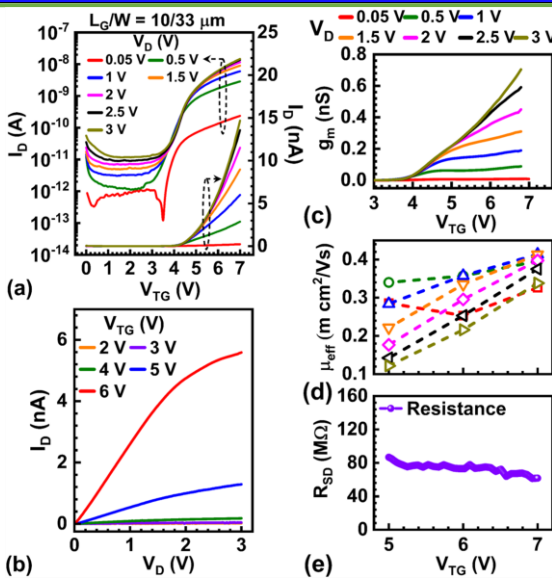


Fig. 5 Measured transfer (a) and output (b) characteristics of the SB MOSFET with top gate control. Extracted (c) g_m , (d) μ_{eff} , and (e) R_{SD} as a function of V_{TG} . Good top gate control is observed. Low on-current is due to SB at S/D as needed for ultra-low power.

Double gate & Scaling

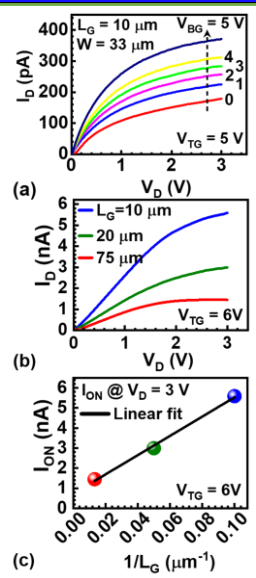


Fig. 6 (a) I_D tunability using V_{BG} at fixed V_{TG} . (b) Device performance with L_G scaling. (c) I_{ON} versus $1/L_G$ shows a linear increase.

Real Time Neuron Demonstration and Spiking Neural Network Performance

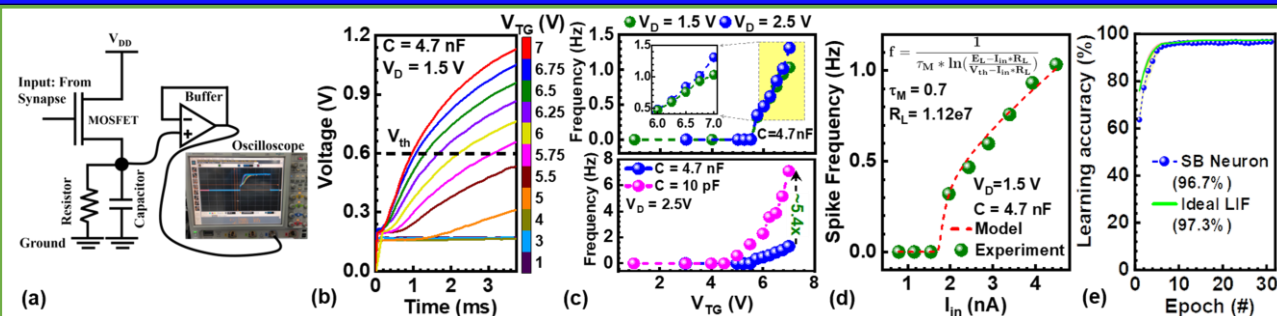


Fig. 7 (a) The circuit used for the neuron demonstration. (b) Measured voltage at capacitor versus time for different V_{TG} at fixed $V_D = 1.5$ V. (c) Frequency versus V_{TG} of a typical neuron for fixed capacitor (C), different V_D , and different C , fixed V_D . Frequency tunability is shown with change in V_D and C values. The observed low frequency is real-time to biology enabled by SB ultra-low current. (d) LIF model response fits with the experimental data. (e) Learning accuracy (maximum=96.7%) on Fisher's Iris data set with the proposed neuron model in MATLAB [3].